ELM and inter-ELM tungsten erosion sources in high-power, JET ITER-like wall H-mode plasmas

H.A. Kumpulainen[a], M. Groth[a], S. Brezinsek[b], G. Corrigan[c], L. Frassinetti[d], D. Harting[c], F. Koechl[c], J. Karhunen[c], A. G. Meigs[c], M. O'Mullane[c], J. Romazanov[b], and JET Contributors[**]

[a]*Aalto University, Espoo, Finland*
[b]*Forschungszentrum Jülich GmbH, Jülich, Germany*
[c]*UKAEA, Culham Science Centre, Abingdon, United Kingdom*
[d]*Division of Fusion Plasma Physics, KTH, Stockholm, Sweden*

henri.kumpulainen@aalto.fi

Abstract

Simulations of JET ITER-like wall high-confinement mode plasmas, including type-I edge-localised modes (ELMs), using JINTRAC for the background plasmas and ERO2.0 for tungsten erosion and transport, predict virtually perfect screening of the primary W erosion sources at the divertor targets during both the ELM and inter-ELM phases. The largest source of W influx to the main plasma is predicted to be the outer vertical divertor due to sputtering by energetic fuel (D, T) atoms from charge-exchange reactions. ERO2.0 predictions accurately reproduce the measured W I emission in the low-field side divertor, but underpredict the W II emission by a factor of 10. Potential reasons for the W II discrepancy include uncertainties in the atomic data, assumptions on the sheath properties and the sputtering angle distribution, and the impact of metastable states.

Keywords: tungsten, erosion, edge-localised mode, JET, JINTRAC, ERO2.0, spectroscopy

**Corresponding author address:* Aalto University, Otakaari 1, 02150 Espoo, Finland

**Corresponding author email:* henri.kumpulainen@aalto.fi

[**]See the author list of 'Overview of JET results for optimising ITER operation' by J. Mailloux et al. to be published in Nuclear Fusion Special issue: Overview and Summary Papers from the 28th Fusion Energy Conference (Nice, France, 10-15 May 2021)

I. Introduction

Tungsten (W) is a promising divertor material choice used in several existing and future tokamaks, such as JET, ASDEX Upgrade, WEST, and ITER, because of its high melting point, high sputtering threshold, and low tritium retention. However, W in the core plasma has a strong detrimental impact on its fusion performance due to radiative energy losses [1]. Hence, understanding and capabilities of predicting W erosion and transport mechanisms are crucial to designing a fusion reactor with W wall components.

The aim of this study is to extend earlier modelling of W sources in JET plasmas [2, 3, 4, 5, 6] to higher-performance scenarios with large type-I edge-localised modes (ELMs), with an emphasis on the validation of the simulated plasma conditions and the plasma-surface interaction models. This is a critical step on the path to validating edge and core plasma impurity transport predictions, as it provides a means to distinguish between uncertainties due to the impurity sources and due to the transport model.

Two series of JET experiments are analysed and modelled in this work: i) diagnostics-optimised tungsten erosion experiments [7] with toroidal magnetic field B_t = 2.5 T, plasma current I_p = 2.5 MA, and auxiliary heating power P_{aux} = 18-20 MW, and ii) hybrid plasma scenarios [8] optimised for fusion performance with B_t = 3.45 T, I_p = 2.2 MA, and P_{aux} = 30-36 MW. Both deuterium and tritium discharges are studied. Further details are provided in Table 1.

II. Setup of JINTRAC and ERO2.0 simulations

Interpretive time-dependent JINTRAC [9] simulations were carried out to obtain background plasmas (BGPs) which simultaneously reproduce the experimentally measured profiles of upstream and low-field side (LFS) target electron density and electron temperature, the upstream ion temperature, and the LFS target ion saturation current as accurately as feasible. The ELMs were modelled using an ad-hoc model [10] with transport multipliers adjusted to reproduce measurements of the ELM-resolved time evolution of pedestal electron density and

electron temperature, plasma stored energy, heat loads on the divertor targets, and the divertor D_α and Be II emission. The purpose of comprehensively fitting the BGPs to measurements was to study uncertainties inherent to W erosion and transport models rather than uncertainties due to an inaccurate BGP.

JINTRAC solutions representing intra-ELM and inter-ELM phases of the ELM cycle were used as BGPs for the ERO2.0 code [11] to predict the W erosion and scrape-off layer (SOL) transport in each ELM phase. Separate pre-ELM and post-ELM phases were used for the hybrid plasma scenarios due to significant time-dependencies in the inter-ELM SOL conditions, whereas a single inter-ELM phase was found to adequately describe both the pre-ELM and post-ELM conditions of the W erosion experiment scenarios.

Inclusion of cross-field drifts in the ELMy BGP simulations was not achieved due to numerical challenges. Drifts were successfully included in an ELM-free scenario, however the best code-experiment agreement was obtained by iteratively adjusting no-drift simulations with ad-hoc cross-field transport. Thus, no-drift BGPs were used. The radial electric field, which is solved by JINTRAC only when drifts are included, was calculated in post-processing for the open flux surfaces using the approximation $E_{rad} \approx -3 \cdot k/e \cdot \partial T_e/\partial r$ [12]. Cross-field drifts are included in the ERO2.0 simulations.

For calculating W erosion by atoms in ERO2.0, the energy-resolved atomic flux densities incident on the plasma-facing components were extracted from EIRENE [13] simulations. Atoms with energies below the W sputtering threshold were discarded from the energy spectra, and the remaining atomic flux densities and their average energies at each wall location were provided as input to ERO2.0. A Maxwellian approximation was used in ERO2.0 for the atomic energy distribution, as the option to import complete atomic energy spectra is yet to be implemented.

The homogeneous material mixing model of ERO2.0 was enabled to allow dynamic surface concentrations of Be and W. The initial surface concentrations for the first time step are based on earlier modelling studies [4] applying the material mixing model to the JET ITER-like

wall [14], as well as on post-mortem tile analysis of JET divertor tiles [15]. A 5 nm thin layer with 70% W – 30% Be composition was assumed near the strike lines, whereas μm-scale deposits of mostly Be were applied in the high-field side (HFS) far SOL and in the private-flux region.

The ERO2.0 version used includes recent improvements, such as a revised model for parallel-B temperature gradient forces based on [16] and corrections to the treatment of the electric field. While based on interpretive BGPs, the W simulations are predictive in the sense that no information from the W measurements was used for fitting, neither in the setup of the BGPs nor in the W simulations.

III. Predicted W density profiles

ERO2.0 predicts that virtually all of the ELM and inter-ELM gross W erosion near the strike line is locally redeposited, either promptly or non-promptly, without affecting the confined plasma (Fig. 1). In contrast, W eroded from the LFS far SOL, primarily due to energetic fuel (D, T) atoms produced by charge-exchange reactions inside the separatrix, is predicted to be poorly screened due to longer ionisation mean-free-paths and weaker plasma flow towards the surfaces. More than 90% of the W influx across the separatrix is predicted to originate from the LFS vertical divertor, despite an order-of-magnitude lower gross W erosion rate compared to the LFS target. The HFS far SOL W surfaces receive net W deposition due to incident plasma flows carrying W from the main chamber SOL.

IV. Comparison of measured and predicted W line emission

The total intensity of 400.9 nm W I emission predicted by ERO2.0 (Fig. 2) at the LFS target is consistent with 2D poloidal tomographic reconstructions [18] of measurements (Fig. 3) using a tangentially-viewing wavelength-filtered divertor endoscope camera [19]. However, ERO2.0 predicts that the emission is more strongly localised at the target than observed. This is likely partially explained by the tomographic reconstruction process not being fully capable of accurately localising the emission along camera lines-of-sight, and partially by a non-negligible

contribution of continuum radiation in the camera images. It is also possible that ERO2.0 predicts W to ionise closer to the targets than in the experiment. The ratio of predicted ELM to inter-ELM W I intensity at the LFS target matches ELM-resolved W I measurements using wavelength-filtered photomultiplier tubes. At the HFS target, code-experiment agreement is not expected due to the no-drift background plasmas being fitted to upstream and LFS target conditions only. The W I emission near the inner strike line is underpredicted due to lower electron temperature in the BGP than in the experiment.

Both ERO2.0 and the camera measurements agree that the W I intensity at the LFS vertical divertor is orders of magnitude weaker than the peak intensity at the LFS target. This does not imply the absence of W erosion (as demonstrated by Fig. 1), because the ratio of emitted W I photons to eroded W atoms is reduced by low electron density and temperature at the LFS vertical divertor.

Line-integrated ERO2.0 predictions match the peak intensity of the measured 400.9 nm W I emission well within measurement uncertainties (Fig. 4a). The measurements are based on a mirror-link visible/near-ultraviolet divertor spectrometer system [17]. The shape of the radial W I emission profile predicted by ERO2.0 is narrower than observed in the experiment, but the ELM-averaged W I intensity is reproduced within approximately a factor of 2 across the entire SOL. Unlike in the 2D tomographic reconstructions, a secondary W I peak is visible in the line-integrated spectrometer signals at R = 2.87 to 2.90 m, corresponding to the LFS vertical divertor. However, the predicted W II emission is lower than measured by a factor of 10 (Fig. 4b), which indicates significant uncertainties in the applied assumptions affecting W^{1+} in ERO2.0 such as the atomic data, including the tracking of metastable states, the sheath model, and the sputtering angle distribution.

V. Sensitivity of W predictions to simulation parameters

Replacing the main ion isotope deuterium with tritium, while otherwise maintaining identical plasma conditions, increases the predicted gross W erosion rate by 90% in both the inter-ELM

and ELM phases. The increased erosion is predominantly sputtering by T ions and atoms, whereas indirect effects such as increased Be and W concentration contributed less than 30% of the predicted isotope effect. Without the assumption of identical plasma conditions, if the BGP conditions are recalculated in JINTRAC for a tritium plasma, ERO2.0 predicts that W erosion in tritium is 100% higher than deuterium in the inter-ELM phase and 120% higher in the ELM phase.

One of the most significant input parameters contributing to uncertainties in the W predictions is the value assigned to the ad-hoc cross-field transport multipliers during ELMs in JINTRAC. Reducing the ELM transport by 20% reduces the predicted intra-ELM erosion rate by one third. On the other hand, scaling the ELM transport by a factor of 1.5 increases the intra-ELM erosion rate by only 15% due to the weak sensitivity of D-on-W sputtering yields to impact energy in the several keV range.

Reducing or increasing the fuelling rate by 20% has a moderate impact of 5–15% on the predicted ELM and inter-ELM gross W erosion rates. A similar 20% change in the input power entering the edge plasma across the core boundary has a more pronounced effect of 20–40%.

Moving from a vertical-horizontal to a corner-corner divertor target configuration, JINTRAC predicts that the inter-ELM target electron temperature is almost doubled. For this reason, the inter-ELM W erosion rate predicted by ERO2.0 in the corner-corner configuration is higher than in vertical-horizontal by a factor of 3. The W erosion predicted in the ELM phase is similar in both configurations. However, due to limited diagnostic coverage of the divertor corners, neither the electron temperature nor the W erosion corner-corner predictions could be conclusively validated against measurements.

Varying the width of the radial outer gap (ROG) between the outer limiter and the mid-plane separatrix from 4 to 8 cm reduces the predicted inter-ELM gross W erosion rate by 25%. This is explained primarily by the slightly lower electron temperature predicted by JINTRAC at the divertor targets. There is also a 30% reduction in the ERO2.0 predicted upstream Be

concentration due to lower incident heat and particle fluxes on Be surfaces, however the ROG has a negligible effect on the measured and predicted Be signals at the LFS target.

The impact of the anomalous cross-field diffusivity of Be and W ions in the range 0.3 to 3.0 m^2/s on the predicted inter-ELM gross W erosion rate is 3%. ERO2.0 predicts marginally higher W sputtering due to Be and W ions with increasing diffusivity.

VI. Conclusions

ERO2.0 simulations of W erosion and SOL transport using type-I ELMy H-mode JINTRAC background plasmas predict W I emission consistent with line-integrated spectrometer measurements and 2D poloidal reconstructions of wavelength-filtered camera images in the JET LFS divertor. However, the W II emission is simultaneously underpredicted by one order of magnitude, which calls for further investigations of assumptions affecting the W^{1+} species in ERO2.0. This is in contrast to earlier work [5], using JINTRAC to predict the W erosion, which reported the opposite discrepancy of overpredicting the W II emission due to the lack of a prompt redeposition model in JINTRAC.

The W screening predicted by ERO2.0 near the strike lines is nearly perfect, whereas erosion by charge-exchange atoms in conjunction with poor screening near the LFS vertical divertor is predicted to be the dominant cause of W influx to the main plasma in both the ELM and inter-ELM phases. The statistical significance of the predicted W influxes could be greatly improved by employing variance reduction techniques, such as particle splitting, to counteract the very high local W redeposition fraction at the divertor targets. More specifically, the few Monte Carlo W particles which avoid local redeposition could be divided into several new Monte Carlo particles to reduce stochastic noise in the main chamber W density predictions.

The ability to predict the W concentration in future plasmas requires not only validated models for W erosion and transport, but also the ability to accurately predict the plasma conditions. Out of the studied parameters, the W erosion rate predicted by ERO2.0 is the most

sensitive to the fuel isotope, the assumed ELM properties, and the input power entering the edge plasma. On the other hand, the value assumed for the impurity cross-field diffusivity, within one order of magnitude, has a negligible impact on the W erosion rate.

Acknowledgements

This work has been carried out within the framework of the EUROfusion Consortium, funded by the European Union via the Euratom Research and Training Programme (Grant Agreement No 101052200 — EUROfusion). Views and opinions expressed are however those of the author(s) only and do not necessarily reflect those of the European Union or the European Commission. Neither the European Union nor the European Commission can be held responsible for them. The ERO2.0 simulations utilised computing resources provided by the Science-IT project at Aalto University.

References

[1] T. Pütterich et al., Nucl. Fusion 50 (2010) 025012.
[2] A. Jaervinen et al., J. Nucl. Mater 438 (2013) S1005-S1009.
[3] D. Harting et al., J. Nucl. Mater 438 (2013) S480-S483.
[4] A. Kirschner et al., Nucl. Mater. Energy 18 (2019) 239-244.
[5] H.A. Kumpulainen et al., Nucl. Mater. Energy 25 (2020) 100866.
[6] M. Navarro et al., 63rd APS DPP Meeting (2021) PO08.00007.
[7] A. Huber et al., Nucl. Mater. Energy 25 (2020) 100859.
[8] L. Garzotti et al., Nucl. Fusion 59 (2019) 076037.
[9] M. Romanelli et al., Plasma Fusion Res. 9 (2014) 3403023.
[10] D. Harting et al., 21st International Conference on Plasma Surface Interactions (2014).
[11] J. Romazanov et al., Nucl. Mater. Energy 18 (2019) 331-338.
[12] P.C. Stangeby, The Plasma Boundary of Magnetic Fusion Devices, Institute of Physics Publishing (2000) ISBN 0 7503 0559 2.
[13] D. Reiter et al., Fusion Science and Technology 47 (2005) 172-186.
[14] G. Matthews et al., Physica Scripta 145 (2011) 014001.
[15] A. Widdowson et al., Nucl. Mater. Energy 19 (2019) 218-224.
[16] Y. Homma et al., Journal of Computational Physics 250 (2013) 206-223.
[17] A. Meigs et al., Review of Scientific Instruments 81 (2010) 10E532.
[18] J. Karhunen et al., Review of Scientific Instruments 90 (2019) 103504.
[19] A. Huber et al., Review of Scientific Instruments 83 (2012) 10D511.

Appendix A

JET pulse #	Time (s)	Description	JINTRAC run IDs	ERO2.0 run IDs
94605	10	W erosion reference	hkumpul/run588s hkumpul/run588g	run02/seq17 run03/seq06
94605	10	D2 fuelling rate -20%	hkumpul/run588t	run16/seq00
94605	10	D2 fuelling rate +20%	hkumpul/run588u	run17/seq00
94605	10	Power to SOL -20%	hkumpul/run588z6	run21/seq00
94605	10	Power to SOL +20%	hkumpul/run588z7	run22/seq00
94605	10	1.5x ELM transport multipliers	hkumpul/run588v	run23/seq00
94605	10	0.8x ELM transport multipliers	hkumpul/run588v3	run29/seq00
94606	11	4 cm wider ROG	hkumpul/run590t	run08/seq01
94606	15	Corner-corner divertor configuration	hkumpul/run591h	run07/seq01
96947	8	Hybrid scenario reference	hkumpul/run098w	run04/seq02
98914	10	Tritium repeat of 94605, P_{aux}=20 MW	hkumpul/run588z9	run20/seq01
99151	8	Tritium repeat of 96947, P_{aux}=31 MW	hkumpul/run099b	run27/seq00

Table 1: Catalogue of JINTRAC simulations stored on the JET Heimdall cluster and ERO2.0 simulations stored on the Aalto University Triton cluster.

a)

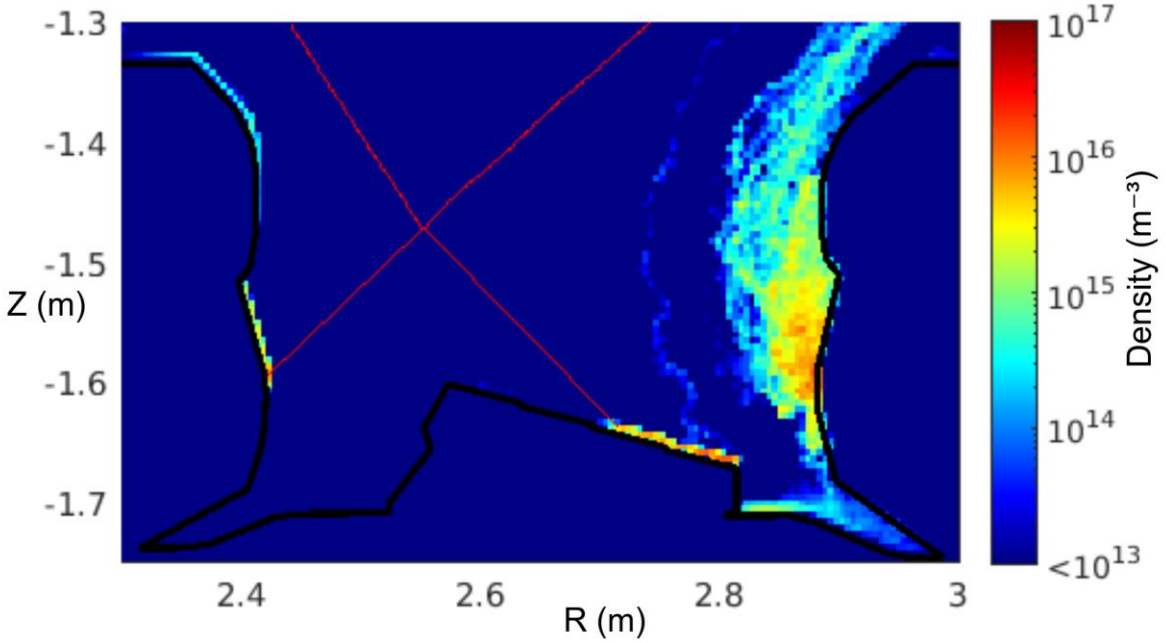

b)

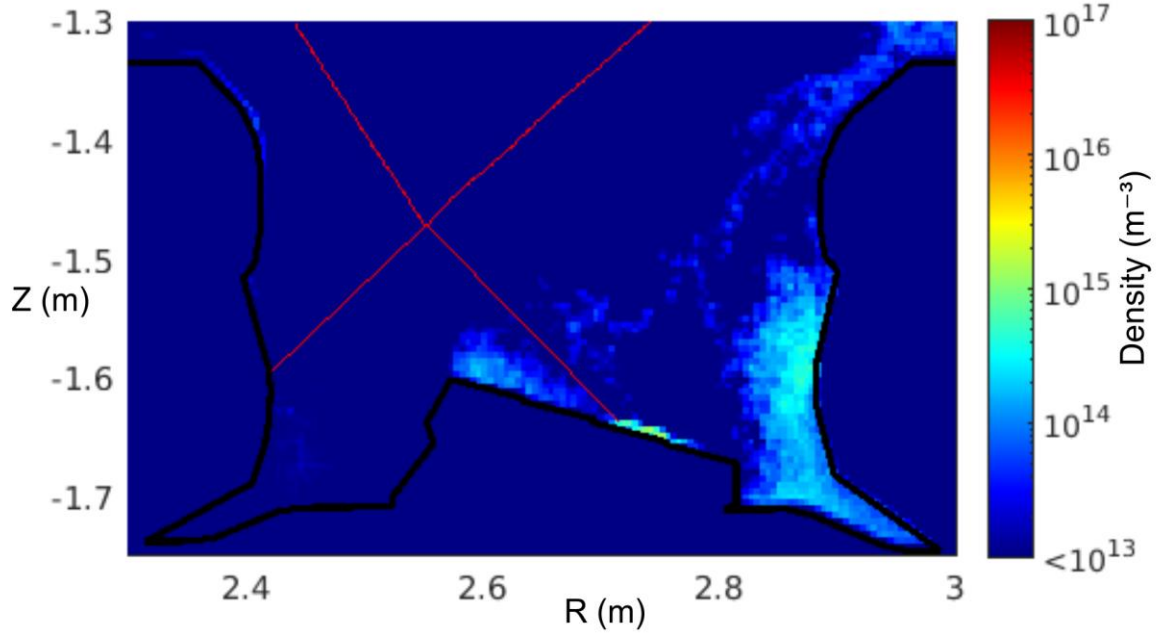

Figure 1: Poloidal cross-sections of W density profiles in the JET divertor predicted by ERO2.0 for steady-state ELM (a) and inter-ELM (b) phases of JPN 94605 (10 s)

a)

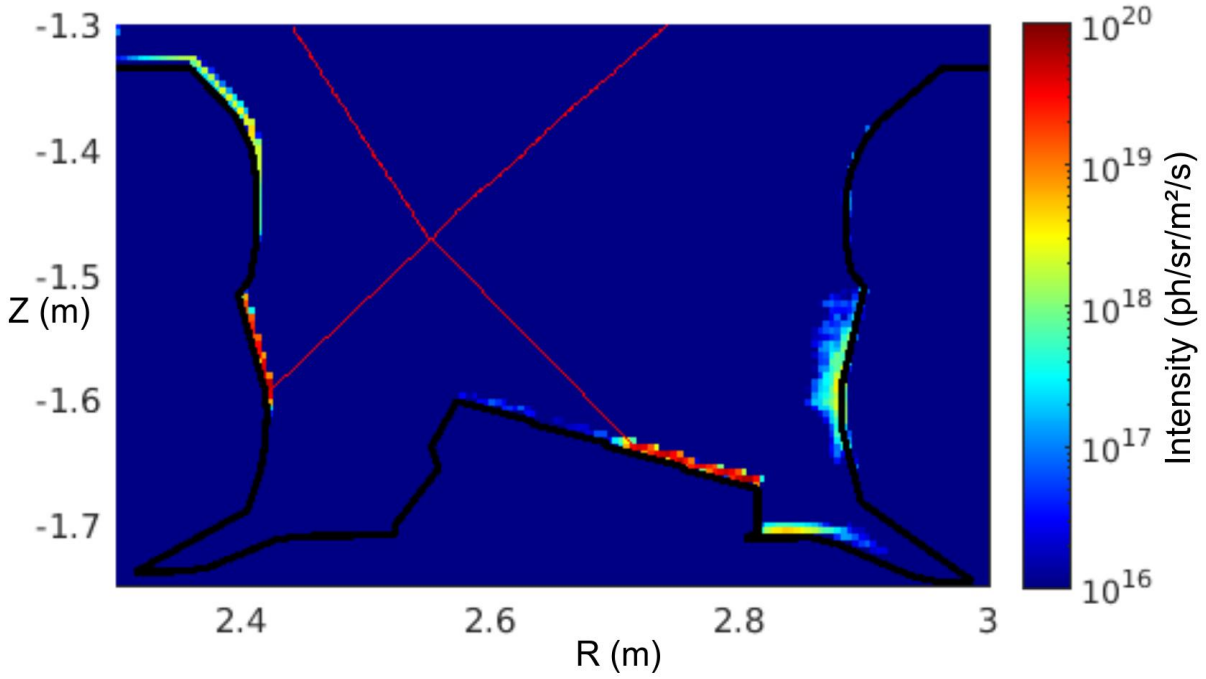

b)

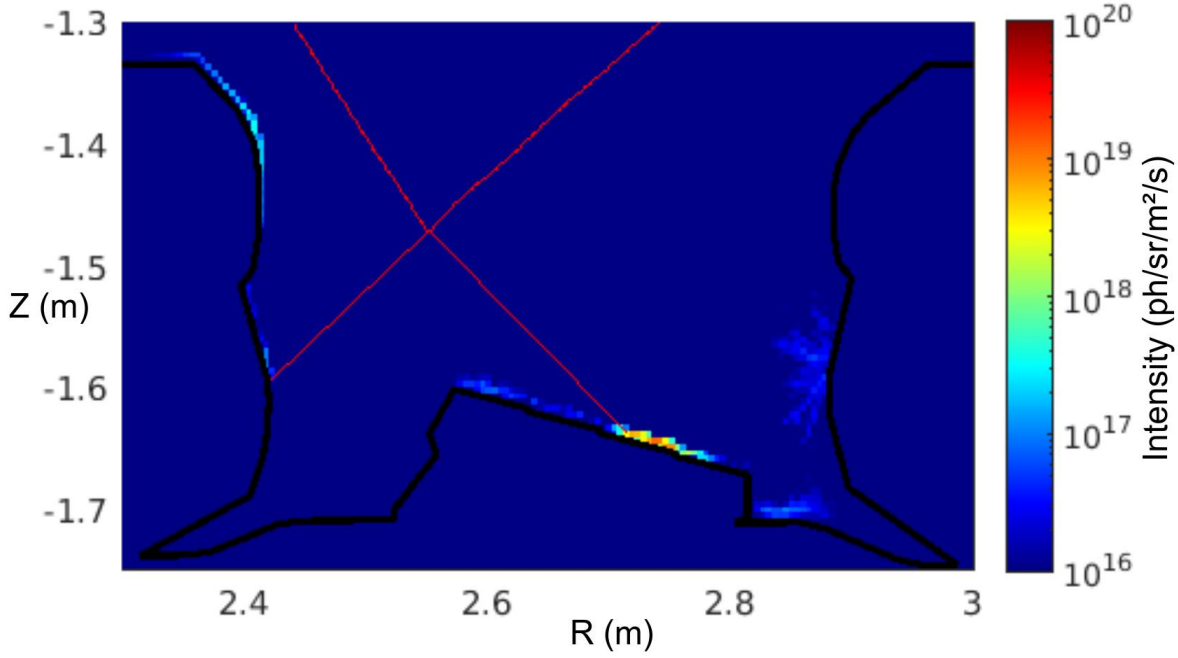

Figure 2: Synthetic reconstructions of the W I 400.9 nm line emission predicted by ERO2.0 for the ELM (a) and inter-ELM (b) phases of JPN 94605 (10 s).

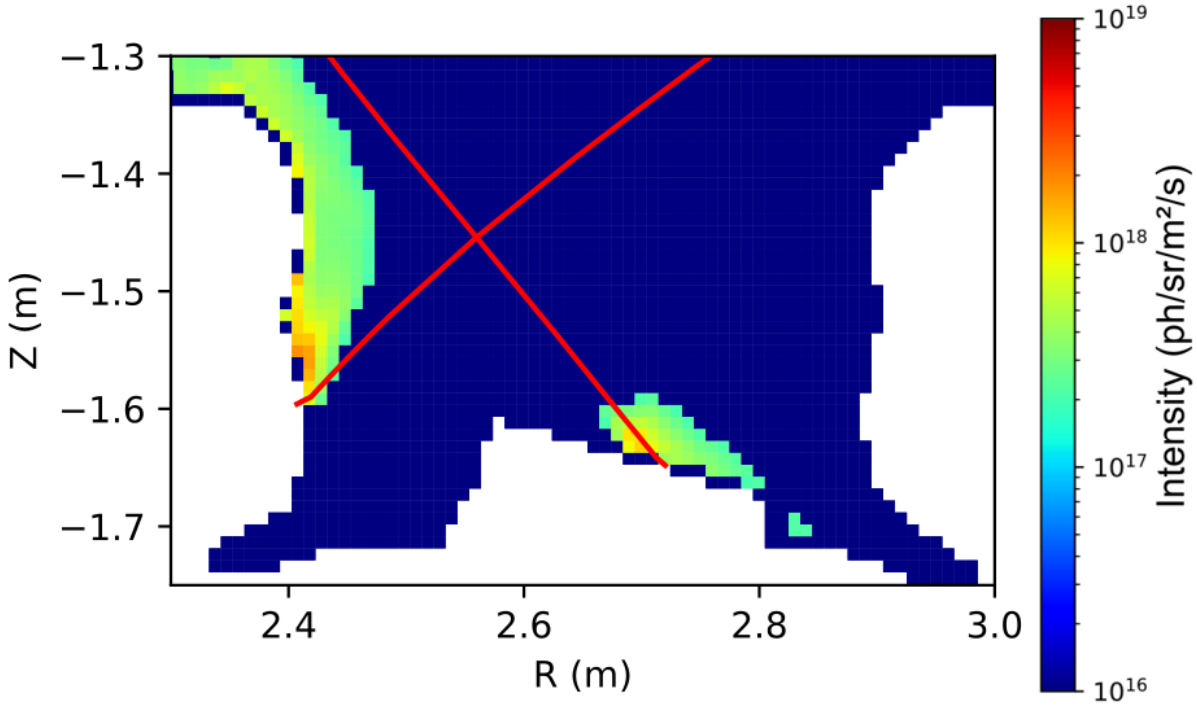

Figure 3: Poloidal tomographic reconstruction of W I 400.9 nm line emission in the JET divertor in JPN 94605 (10 s) measured using a tangentially viewing endoscope camera equipped with a wavelength filter. Intensities below $2 \cdot 10^{17}$ ph $sr^{-1}m^{-2}s^{-1}$ are masked to zero due to significant contributions from continuum radiation.

a)

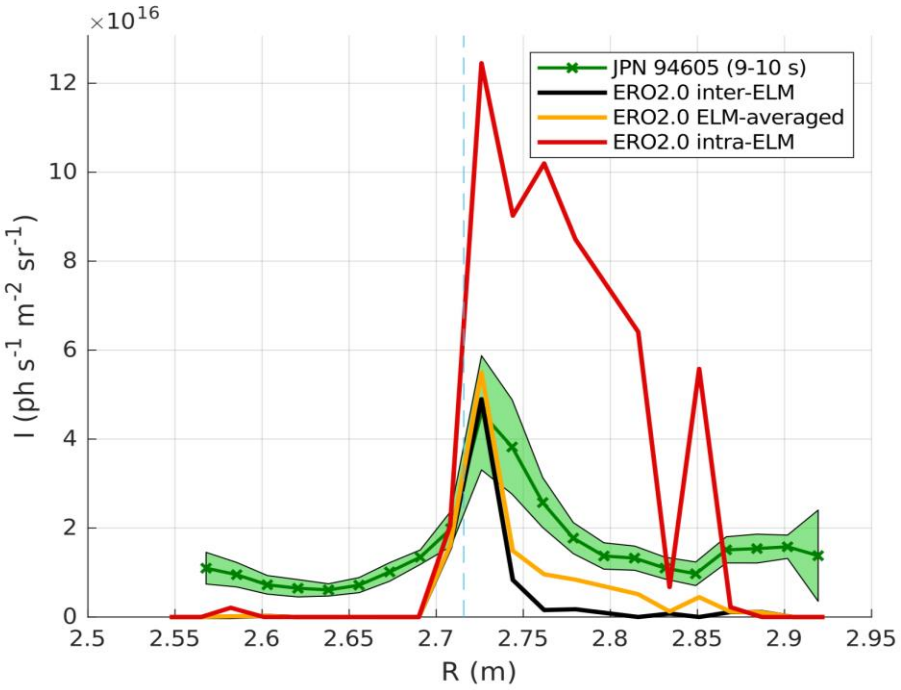
×10^16
12
10
8
6
4
2
0
I (ph s^-1 m^-2 sr^-1)
2.5
2.55
2.6
2.65
2.7
2.75
2.8
2.85
2.9
2.95
R (m)
JPN 94605 (9-10 s)
ERO2.0 inter-ELM
ERO2.0 ELM-averaged
ERO2.0 intra-ELM

b)

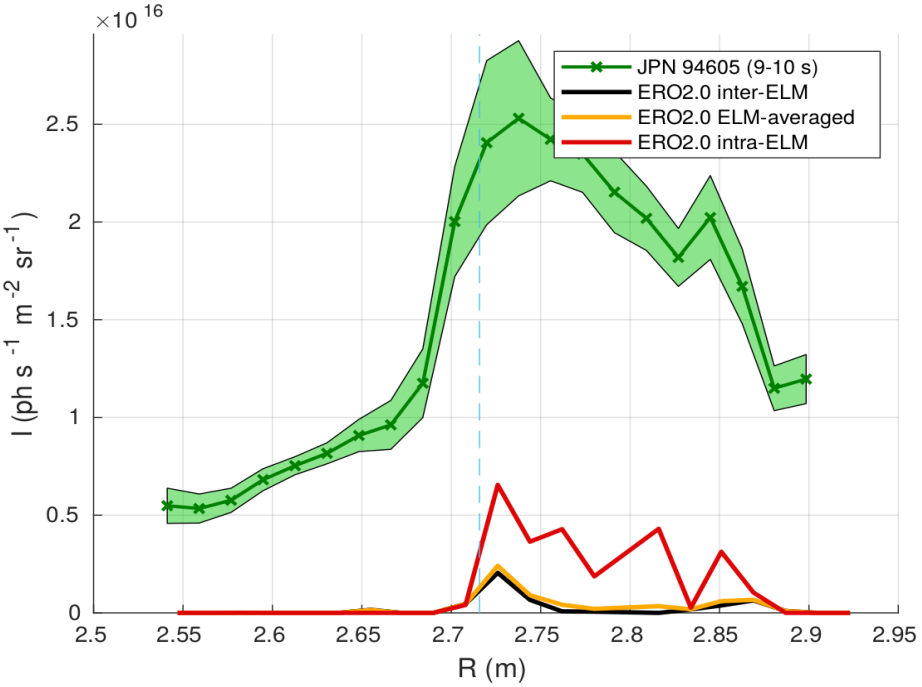
×10^16
2.5
2
1.5
1
0.5
0
I (ph s^-1 m^-2 sr^-1)
2.5
2.55
2.6
2.65
2.7
2.75
2.8
2.85
2.9
2.95
R (m)
JPN 94605 (9-10 s)
ERO2.0 inter-ELM
ERO2.0 ELM-averaged
ERO2.0 intra-ELM

Figure 4: Line-integrated W I 400.9 nm emission (a) and W II 434.8 nm emission (b) in the JET low-field side divertor in JPN 94605 (9-10 s) measured by a mirror-link Czerny-Turner divertor spectrometer (green, with shaded area indicating one standard deviation) and predicted by ERO2.0 for the inter-ELM (black) and intra-ELM (red) phases. The duration-weighted ELM-averaged W I intensity, assuming an ERO2.0 ELM cycle with 2 ms ELM duration and 40 Hz frequency, is shown in orange. The vertical dashed blue line indicates the radial location of the strike line.